

Magnesium-binding studies reveal fundamental differences between closely related RNA triphosphatases

Marie F. Soulière, Jean-Pierre Perreault and Martin Bisailon*

Département de Biochimie, RNA Group, Faculté de Médecine, Université de Sherbrooke, Sherbrooke, Québec J1H 5N4, Canada

Received September 7, 2007; Revised November 11, 2007; Accepted November 12, 2007

ABSTRACT

The *Chlorella* virus RNA triphosphatase (cvRTPase) is involved in the formation of the RNA cap structure found at the 5'-end of the viral mRNAs and requires magnesium ions to mediate its catalytic activity. To extend our studies on the role of metal ions in phosphohydrolysis, we have used a combination of fluorescence spectroscopy, circular dichroism, denaturation studies and thermodynamic analyses to monitor the binding of magnesium ions to the cvRTPase. Using these techniques, the thermodynamic forces responsible for the interaction of metal ions with an RNA triphosphatase were also evaluated for the first time. Our thermodynamic analyses indicate that the initial association of magnesium with the cvRTPase is dominated by a favorable entropic effect and is accompanied by the release of eight water molecules from the enzyme. Moreover, both fluorescence spectroscopy and circular dichroism assays indicated that minor conformational changes were occurring upon magnesium binding. Mutational studies were also performed and confirmed the importance of three specific glutamate residues located in the active site of the enzyme for the binding of magnesium ions. Finally, in contrast to the yeast RNA triphosphatase, we demonstrate that the binding of magnesium ions to the cvRTPase does not lead to the stabilization of the ground state binding of the RNA substrate. Based on the results of the present study, we hypothesize that the binding of magnesium ions induces local conformational perturbations in the active site residues that ultimately positions the lateral chains of critical amino acids involved in catalysis. Our results highlight fundamental differences in the role of magnesium ions

in the phosphohydrolyase reactions catalyzed by the cvRTPase and the closely related yeast RNA triphosphatase.

INTRODUCTION

The synthesis and maturation of eukaryotic mRNAs are crucial events for gene expression. Following mRNA synthesis, eukaryotic mRNAs undergo a series of critical modifications before being exported to the cytoplasm where they are translated into proteins (1). These processing events include the addition of a cap structure at the 5' terminus, the splicing out of introns, the editing of specific nucleotides and the acquisition of a poly(A) tail at the 3' terminus. The eukaryotic cap structure found at the 5' end of mRNAs is critical for translation, stability and transport of mRNAs from the nucleus to the cytoplasm (2,3). Synthesis of the cap structure occurs co-transcriptionally on nascent mRNAs and involves three enzymatic reactions (2,3). First, an RNA 5'-triphosphatase hydrolyses the γ phosphate at the 5'-end of the nascent pre-mRNA to generate a 5'-diphosphate end. An RNA guanylyltransferase then transfers a GMP moiety to the diphosphate end of the RNA. Finally, an RNA (guanine-7) methyltransferase catalyzes the transfer of a methyl group to the N-7 position of the guanine to produce the characteristic m⁷GpppRNA cap structure.

A number of different viruses use the enzymes of the cell that they infect to synthesize the cap structure found at the 5' ends of the viral mRNAs. Such is the case for herpes viruses, parvo viruses, papova viruses and adeno viruses. Interestingly, several viruses including poxviruses, reoviruses, alphaviruses, baculoviruses, West Nile virus and *Chlorella* virus PBCV-1 encode for their own enzymes which are involved in the synthesis of a cap structure (4–9). Although the RNA cap structures originating from viral and cellular enzymes are often identical, the physical organization of the genes, subunit composition, structure and catalytic mechanisms of the virus-encoded enzymes

*To whom correspondence should be addressed. Tel: +(819) 564 5227; Fax: +(819) 564 5340; Email: martin.bisailon@usherbrooke.ca

involved in the synthesis of the RNA cap structure are significantly different from those of host cells (2). As a consequence these viral cap-forming enzymes are potential targets for antiviral drugs that would inhibit the capping of viral mRNAs (10–12).

Two families of RNA triphosphatases have been identified through the purification and characterization of mammalian, yeast, protozoan and viral enzymes. The first family consists of RNA triphosphatases from metazoans and plants that possess the ability to catalyze the hydrolysis of the γ -phosphate of mRNAs (13,14). These metal-independent enzymes belong to the cysteine phosphatase family and catalyze a two-step reaction that involves a covalent cysteinyl-phosphoenzyme intermediate (13,14). The second family of RNA triphosphatases, encompassing metal-dependent enzymes from fungi, viruses, protozoan and microsporidian parasites, is characterized by three collinear motifs that include amino acids that are essential for activity (13,15–18). Catalysis by these enzymes involves the attack of a water molecule in close proximity to the γ -phosphate with no formation of a covalent intermediate (19). Analysis of the crystal structure of both the *Saccharomyces cerevisiae* (19) and mouse RNA triphosphatases (20), in conjunction with the recent crystallization of the baculovirus RNA triphosphatase (21), has brought new insights into the enzymatic reactions catalyzed by these metal-dependent proteins. For instance, the structure of the *S. cerevisiae* enzyme revealed a distinctive active site that is characterized by an eight-stranded β -barrel that defines a topologically closed tunnel (19). Based on the crystal structure, a catalytic mechanism has been proposed in which the essential acidic amino acids located on the base of the tunnel would coordinate the essential divalent cation that is adjacent to the γ -phosphate (19). The essential divalent cation would allow the activation of the γ -phosphate for attack by water, and the stabilization of a pentacoordinate phosphorane transition state (19). Moreover, amino acids located on the walls and roof of the tunnel appear to contribute to the coordination of the γ -phosphate, and to the stabilization of the negative charge on the γ -phosphate that arises during the formation of the transition state (19).

Chlorella virus PBCV-1 is the prototype of a family of large icosahedral DNA viruses that replicate in the unicellular *Chlorella*-like green algae (22). Analysis of the enzyme revealed that the *Chlorella* virus RNA triphosphatase (*cv*RTPase) is more closely related to the cellular triphosphatases of fungi (*S. cerevisiae*) than to other DNA virus-encoded RNA triphosphatases (23,24). Mutational data suggest that its active site is located within a tunnel similar to that of *S. cerevisiae* and that the amino acids involved in catalysis are similar in both enzymes (23,24). However, differences in structure–activity relationships suggest the existence of subtle mechanistic distinctions between the metal-dependent *Chlorella* virus and fungal RNA triphosphatases (24).

As a first step toward elucidating the nature and the role(s) of the metal ion cofactors in the RNA triphosphatase reaction, we had initially characterized the binding of metal ions to the *S. cerevisiae* RNA

triphosphatase (25). Metal ions were shown to be critical for the stabilization of the ground state binding of the phosphohydrolyase substrate (25). Structural studies also showed that the binding of the metal cofactor did not lead to significant structural modifications of the architecture of the yeast RNA triphosphatase (25). Here, we extend our analysis on the role of metal ions in the RNA triphosphatase reaction by evaluating the interactions of magnesium ions with the *cv*RTPase. Using a combination of fluorescence spectroscopy, circular dichroism and denaturation studies, we correlated the effect of metal ion binding on the structure and stability of the enzyme. Moreover, the thermodynamic forces responsible for the interaction of magnesium with the RNA triphosphatase were also evaluated. Our results highlight fundamental differences in the role of metal ions in the reactions catalyzed by the *Chlorella* virus and yeast RNA triphosphatases.

MATERIALS AND METHODS

*cv*RTPase expression and purification

The *cv*RTPase was expressed and purified as described previously (26).

Fluorescence measurements

Fluorescence was measured using an Hitachi F-2500 fluorescence spectrophotometer. Background emission was eliminated by subtracting the signal from either buffer alone or buffer containing the appropriate quantity of substrate.

The extent to which ligands bind to the *cv*RTPase was determined by monitoring the fluorescence emission of a fixed concentration of proteins and titrating with a given ligand. The binding can be described by Equation (1),

$$K_D = \frac{[cvRTPase][ligand]}{[cvRTPase \times ligand]} \quad 1$$

where K_D is the apparent dissociation constant, $[cvRTPase]$ is the concentration of the protein, $[cvRTPase \times ligand]$ is the concentration of complexed protein and $[ligand]$ is the concentration of unbound ligand in solution. The proportion of ligand-bound protein, as described by Equation (1), is related to measured fluorescence emission intensity by Equation (2),

$$\frac{\Delta F}{\Delta F_{max}} = \frac{[cvRTPase \times ligand]}{[cvRTPase]_{tot}} \quad 2$$

where ΔF is the magnitude of the difference between the observed fluorescence intensity at a given concentration of ligand and the fluorescence intensity in the absence of ligand, ΔF_{max} is the difference at infinite $[ligand]$, and $[cvRTPase]_{tot}$ is the total protein concentration.

If the total ligand concentration, $[ligand]_{tot}$, is in large molar excess relative to $[cvRTPase]_{tot}$, then it can be assumed that $[ligand]$ is approximately equal to $[ligand]_{tot}$.

Equations (1) and (2) can then be combined to give Equation (3).

$$\frac{\Delta F}{\Delta F_{\max}} = \frac{[\text{ligand}]_{\text{tot}}}{(K_D + [\text{ligand}]_{\text{tot}})} \quad 3$$

The K_D values were determined from a nonlinear least square regression analysis of titration data by using Equation (3), and the stoichiometry of binding was established from a linear version of the Hill equation [Equation (4)],

$$\log \left[\frac{\Delta F}{(\Delta F_{\max} - \Delta F)} \right] = n \log[\text{ligand}] - \log K' \quad 4$$

where n is the order of the binding reaction with respect to ligand concentration and K' is the concentration of ions that yields 50% of ΔF_{\max} . Finally, the Gibbs free energy of binding was established using Equation (5),

$$\Delta G = -RT \ln K_A \quad 5$$

where R is the gas constant, T is the temperature and K_A is the association constant ($K_A = 1/K'$).

Circular dichroism spectroscopy measurements

Circular dichroism measurements were performed with a Jasco J-810 spectropolarimeter. The samples were analyzed in quartz cells with path lengths of 1 mm. Far-UV and near-UV wavelength scans were recorded from 200 to 250 nm and from 250 to 340 nm, respectively. All the CD spectra were corrected by subtraction of the background for the spectrum obtained with either buffer alone or buffer containing the ligand. The average of three wavelength scans is presented. The ellipticity results were expressed as mean residue ellipticity, $[\theta]$, in degrees cm^2/dmol .

Thermal unfolding experiments

Thermal denaturations were monitored by following the change in CD ellipticity of the *cv*RTPase protein (2 μM) at 222 nm. The samples were heated from 20°C to 90°C, at a heating rate of 1°C/min. The ellipticity results were expressed as mean residue ellipticity, $[\theta]$, in degrees cm^2/dmol . The fraction of unfolded protein at each temperature was determined by calculating the ratio $[\theta_{222}]/[\theta_{222}]_d$, where $[\theta_{222}]_d$ is the molar ellipticity for the completely unfolded enzyme.

Equilibrium unfolding experiments

For all unfolding experiments, a 2 μM solution of purified *cv*RTPase was adjusted to the desired final concentration of guanidium hydrochloride (Gdm-HCl) and incubated for 60 min at 25°C. The intrinsic fluorescence of the protein was then monitored as a function of the Gdm-HCl concentration. The parameters ΔG_u (Gibbs free energy of unfolding), ΔG_u^0 (Gibbs free energy of unfolding in the absence of denaturant), m (cooperativity of unfolding) and C_m (midpoint concentration of denaturant required to unfold 50% of the

protein) were obtained as previously outlined (27) using Equations (6) and (7).

$$\Delta G_u = -RT \ln K_u \quad 6$$

$$\Delta G_u = \Delta G_u^0 - m[\text{Gdm} - \text{HCl}] \quad 7$$

Quenching of the *cv*RTPase by acrylamide

Quenching experiments were performed at 25°C by adding increasing concentrations of acrylamide. The excitation wavelength was set at 290 nm, and the fluorescence emission spectra were scanned from 300 to 400 nm. The integration area between 330 and 360 nm was used for data analysis. The fluorescence quenching data in the presence of acrylamide were analyzed according to the Stern–Volmer equation (28),

$$\frac{F_0}{F} = 1 + K_{sv}[Q] \quad 8$$

where F_0 and F are the fluorescence intensities in the absence or presence of the quencher, respectively. K_{sv} is the dynamic Stern–Volmer quenching constant, and $[Q]$ is the quencher concentration.

When the Stern–Volmer displayed an upward curvature, the static quenching concept was used, and the experimental data were fitted to a revised Stern–Volmer equation,

$$\frac{F_0}{F} = (1 + K_{sv}[Q])e^{V[Q]} \quad 9$$

where V is the static quenching constant measuring the complex formation between acrylamide and the enzyme.

Thermodynamics of binding

The temperature dependence of the association constants (K_A) for ligand binding was analyzed according to the van't Hoff isobaric equation, assuming that the entropy change (ΔS°) and the enthalpy change (ΔH°) remained constant over the whole range of temperatures [Equation (10)].

$$\ln K_A = \frac{\Delta S^\circ}{R} - \frac{\Delta H^\circ}{RT} \quad 10$$

ANS binding measurements

Binding of ANS (1-anilino-8-naphthalenesulfonate) was evaluated by measuring the fluorescence enhancement of ANS (50 μM) upon excitation at a wavelength of 380 nm. The emission spectra were integrated from 400 to 600 nm.

Release of water molecules during binding of magnesium ions

The binding of magnesium ions was measured in the presence of different osmolal concentrations using either glycerol or ethylene glycol as the neutral solutes. The respective binding free energies were then evaluated from Equation (5). As reported previously (29), the

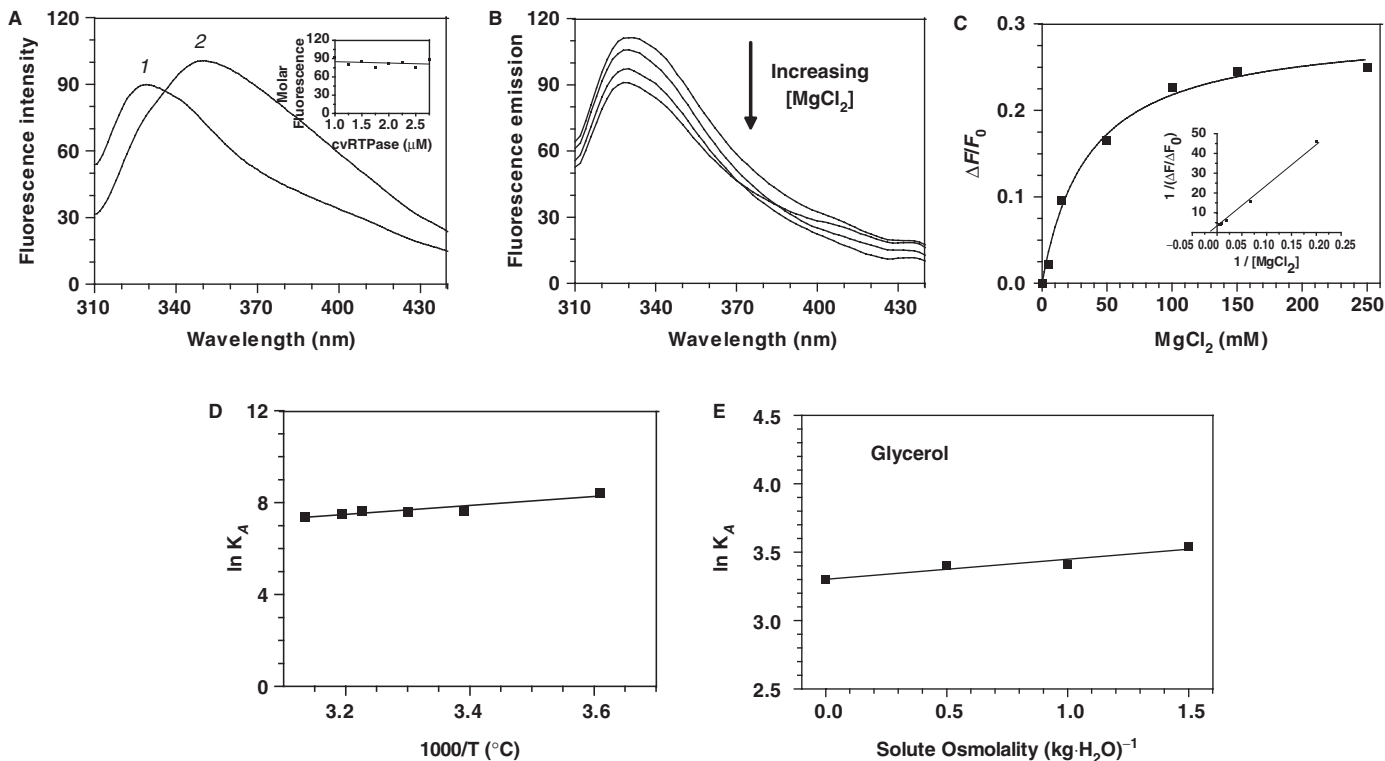


Figure 1. Binding of magnesium ions to the *cvRTPase*. (A) Background corrected fluorescence emission spectra of the *cvRTPase*. 1, Purified protein in 50 mM Tris-HCl, and 50 mM KOAc, pH 7.5; 2, Purified protein after a 2 h exposure to an 8 M solution of urea at 25°C. Fluorescence spectra were recorded at an excitation wavelength of 290 nm. The molar fluorescence of the enzyme is shown in inset. Various concentrations of the purified protein were assayed in 50 mM Tris-HCl, and 50 mM KOAc, pH 7.5. Emission was monitored at 333 nm and excitation was performed at 290 nm. (B) Increasing amounts of magnesium ions were added to a 1 μ M solution of the enzyme in binding buffer (50 mM Tris-HCl and 50 mM KOAc, pH 7.5) and the emission spectrum was scanned from 310 to 440 nm. (C) A saturation isotherm can be generated from these data by plotting the change in fluorescence intensity at 333 nm as a function of added magnesium ions. A double-reciprocal plot is shown in the inset. (D) Thermodynamic parameters of the interaction between magnesium and the *cvRTPase*. Binding assays were performed at various temperatures. A van't Hoff plot for the interaction between magnesium and the enzyme is shown. The effect of temperature on the association constant was evaluated at pH 7.0. (E) The effect of a neutral solute (glycerol) on the binding of magnesium to the *cvRTPase* was analyzed. The binding parameters were evaluated at pH 7.0.

slope of $\ln K_A$ versus $[\text{solute}]_{\text{osmolality}}$ can then be used to evaluate the number of water molecules that are released upon ligand binding according to Equation (11),

$$\frac{d \ln K_A}{d[\text{solute}]_{\text{osmolality}}} = \frac{-\Delta n_w}{55.56} \quad 11$$

where Δn_w is the number of water molecules that are released during the binding process, and the 55.56 value is the moles of water found in 1 kg.

RESULTS

Metal ion binding activity of *cvRTPase*

Magnesium is the metal ion cofactor, which is used by the *cvRTPase* to mediate the hydrolysis of the γ -phosphate found at the 5'-terminus of nascent mRNAs (23,24). Fluorescence emission spectroscopy was used to monitor the direct binding of magnesium ions to the purified enzyme. The fluorescence emission spectrum of the purified enzyme in standard buffer at 25°C is shown in Figure 1A. The emission maximum of the enzyme (333 nm) is blue-shifted relative to that of free

L-tryptophan (Figure 1A), which under the same conditions is observed to be at 350 nm. Blue shifts of protein emission spectra have been ascribed to shielding of the tryptophan residues from the aqueous phase due to the three-dimensional structure of the protein (30). Accordingly, denaturation of the protein with 8.0 M urea results in a red shift of λ_{max} towards 350 nm (Figure 1A). Analysis of the molar intensity of the fluorescence emission spectrum of the *cvRTPase* revealed a linear change of 2.2 fluorescence intensity units/ μ M of protein (Figure 1A). This relatively small change can probably be attributed to small losses of proteins from solution through minor aggregation that occurs at higher protein concentrations. All subsequent binding experiments were therefore performed at a protein concentration of 1 μ M, with the assumption that the binding equilibrium was not complicated by the presence of an aggregation equilibrium.

Increasing amounts of magnesium were then added to the purified *cvRTPase* protein, and the fluorescence intensity was monitored. We observed that the binding of magnesium ions resulted in a decrease in the fluorescence intensity of the enzyme (Figure 1B).

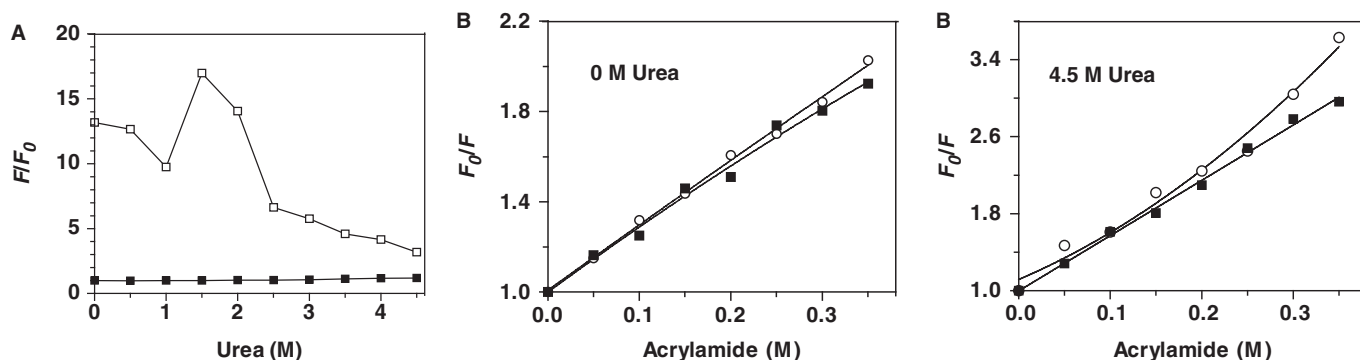


Figure 2. Effect of magnesium ions on the structure of the enzyme. (A) Binding of ANS to the *cvRTPase* during urea denaturation. The *cvRTPase* was incubated in the absence (filled square) or presence (open square) of 50 mM $MgCl_2$, and unfolded with various concentrations of urea at 25°C for 1 h. Fluorescence emission was monitored after ANS addition (50 μ M) at an excitation wavelength of 380 nm. The integrated fluorescence area between 400 and 600 nm was evaluated. (B and C) Stern–Volmer plots for the quenching of the intrinsic fluorescence of the *cvRTPase* by acrylamide. The *cvRTPase* was incubated in the absence (filled square) or presence (open square) of 50 mM $MgCl_2$, and denatured with (B) 0 M, (C) 4.5 M urea at 25°C for 1 h. The denatured enzyme was then titrated with various amounts of acrylamide. Excitation was set at 290 nm, and the emission of the fluorescence-integrated area between 320 and 370 nm was determined.

However both the emission maximum and spectral bandwidth were not significantly affected. About 28% of the intrinsic protein fluorescence was accessible to the quencher magnesium ions (Figure 1C). As a consequence, we were able to evaluate the binding parameters by titrating the binding of increasing amounts of metal ions to a fixed concentration of the enzyme. Our binding studies indicate that the Gibbs free energy of binding (ΔG) for the interaction of magnesium with the enzyme was -8.2 kJ/mol. Analysis of a Hill plot, generated from the Mg^{2+} ion binding data, yielded a Hill coefficient of 1.2, indicating a lack of cooperativity (Supplementary Figure 1A). Furthermore, a Scatchard plot of Mg^{2+} binding data is linear, providing no evidence for multiple classes of independent magnesium ion binding sites, nor of cooperative binding sites (Supplementary Figure 1B).

Although the free energy of binding provides the overall description of the system, defining the entropic and enthalpic contributions to the free energy provides a more complete understanding of the forces that drive the protein–RNA association. The enthalpic (ΔH) and entropic contributions ($T\Delta S$) to the free energy of binding ($\Delta G = \Delta H - T\Delta S$) were evaluated by determining the temperature dependence of the association constant (K_A) for magnesium ions (Figure 1D). The magnesium binding reaction was shown to be exothermic at 25°C with an enthalpy of association of $\Delta H = -2.5$ kJ/mol. Analysis of a van't Hoff plot for the interaction between magnesium and the *cvRTPase* (Figure 1D) revealed that the $T\Delta S$ value for the binding reaction was 5.7 kJ/mol, clearly indicating that the initial metal ion binding step is primarily driven by entropy. Furthermore, the binding reaction is clearly favorable with the resultant $\Delta S^\circ = 19$ J/mol K.

We next sought to investigate if the binding of magnesium to the *cvRTPase* could be accompanied by the release of water molecules in the solvent. The dependence of the thermodynamic parameters for the binding of magnesium on the osmolal concentration of the neutral solute glycerol was then investigated.

As shown in Figure 1E, the binding free energy shows a linear dependence on the solute osmolal concentration. This is consistent with an exclusion of the solute molecules (glycerol) upon formation of the *cvRTPase*–Mg complex. The positive sign of the slope defines the net release of water molecules that occurs during the process of binding. From a fit of Equation (11), our results indicate that eight water molecules ($\Delta n_w = 8.1$) are released from the *cvRTPase* upon binding of magnesium. Note that a similar value of eight water molecules ($\Delta n_w = 7.7$) was also obtained when ethylene glycol was substituted for glycerol as the neutral solute (Supplementary Figure 1C).

Finally, in order to evaluate the contribution of the electrostatic interactions in the formation of the *cvRTPase*–Mg complex, binding assays were performed in the presence of increasing ionic strength. The data revealed that interaction between the enzyme and magnesium is insensitive to ionic strength as similar ΔG values were observed in the presence of high concentrations of KCl (Supplementary Figure 1D). Therefore, it appears that electrostatic interactions are not making a significant contribution to the overall binding energy.

Effect of magnesium ions on the structure of the enzyme

Structural studies performed with the closely related RNA triphosphatase of *S. cerevisiae* previously revealed that the binding of metal ions does not lead to significant structural modifications of the yeast enzyme (25). We therefore intended to monitor potential structural modifications that could occur in the *cvRTPase*. The exposure of hydrophobic areas of the *cvRTPase* was evaluated by measuring the binding of ANS, which interacts with hydrophobic patches on the surface of the protein, resulting in an enhancement of ANS intrinsic fluorescence (31). Our data revealed that the unliganded enzyme binds very weakly to ANS, probably reflecting limited hydrophobic regions at the surface of the protein (Figure 2A). However, a significant increase of the ANS fluorescence is observed when the protein is incubated in the presence of saturating concentrations of

Table 1. Quenching of the *cv*RTPase intrinsic fluorescence by acrylamide

Urea concentration	<i>V</i>		<i>K_{sv}</i>	
	-Mg ²⁺	+Mg ²⁺	-Mg ²⁺	+Mg ²⁺
M	M ⁻¹		M ⁻¹	
0	1.000	1.008	2.972	2.919
1.0	0.991	1.023	2.163	2.203
2.0	0.968	0.985	3.266	3.273
4.5	1.117	0.998	4.063	5.731
6.0	1.022	0.993	5.772	8.081

Fluorescence spectroscopy assays were performed to evaluate both the dynamic Stern-Volmer quenching constant (*K_{sv}*) and the static quenching constant (*V*). The quenching experiments were performed both in the absence (-Mg²⁺) or in the presence (+Mg²⁺) of 50 mM Mg²⁺.

magnesium ions (Figure 2A). As expected, increasing the urea concentrations resulted in a drastic decrease of the emission intensity, as the protein with bound Mg²⁺ became unfolded by the denaturant. Overall, these data indicate that magnesium ion binding increases hydrophobic exposure on the surface of the *cv*RTPase. Circular dichroism studies also confirmed that minor structural modifications are occurring upon magnesium binding (Supplementary Figure 2A and B).

To better understand the conformational changes that occur following the binding of magnesium ions to the *cv*RTPase, quenching experiments were performed in the presence of acrylamide. Acrylamide is a non-selective quencher of proteins that can penetrate into the interior of the protein matrix (32). Our binding studies show that in the absence of denaturant, no significant differences were observed between the unliganded enzyme and the enzyme bound to magnesium (Figure 2B). The acrylamide quenching experiments were then performed in the presence of increasing urea concentrations and, as seen in Figure 2B, the unliganded enzyme was significantly more sensitive to acrylamide quenching when the protein was denatured with high concentrations of urea. This sensitivity was particularly evident in the presence of 2.0 and 4.5 M urea, where the binding of Mg²⁺ ions clearly destabilized the protein and promoted the quenching of the enzyme by acrylamide (Figure 2C and Table 1). Overall, the acrylamide quenching assays performed in the presence of increasing urea concentrations indicate that magnesium ion binding to the *cv*RTPase significantly decreases the structural stability of the protein.

Thermodynamic stability

To further investigate the destabilizing effect of magnesium on the protein architecture, Gdm-HCl-induced denaturation studies were performed. The intrinsic fluorescence of the enzyme was monitored in the presence of increasing concentrations of Gdm-HCl. We observed a quenching of the intrinsic fluorescence intensity and a red shift in the emission maximum, reflecting the transfer of tryptophan residues to a more polar environment (data not shown). The change of the integrated

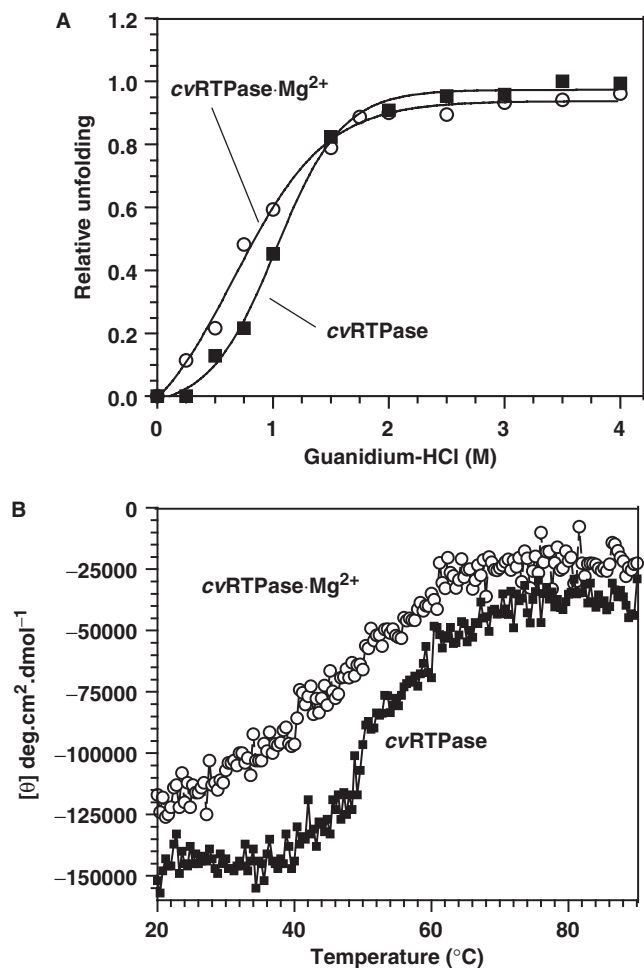


Figure 3. Structural consequences of magnesium binding to the *cv*RTPase. (A) Transition curves for Gdm-HCl-induced unfolding of the *cv*RTPase were monitored both in the absence (filled square) or presence of 50 mM of Mg²⁺ (open circle). Equilibrium unfolding transitions were monitored by integration of the fluorescence intensity. (B) Thermal denaturation of the *cv*RTPase enzyme. Thermal denaturation was recorded for the unliganded protein (filled square), or the protein incubated in the presence of 50 mM MgCl₂ (open circle). Circular dichroism spectra were recorded at a constant wavelength of 222 nm from 20°C to 90°C at a protein concentration of 2 μM.

fluorescence intensity as a function of the Gdm-HCl concentration is shown in Figure 3A. The *cv*RTPase structure reacts very sensitively to the slightest concentration changes in the lower concentration range between 0.5 and 1.5 M where the strongest effects on emission changes are observed. No radical changes could be seen at Gdm-HCl concentrations higher than 2.5 M. The protein displays a smooth transition curve, indicating a cooperative unfolding event. The thermodynamic unfolding parameters were determined and are presented in Table 2. The denaturation experiments were then carried out in the presence of magnesium to evaluate if the binding of metal ions could modify the stability of the protein. Incubation of the enzyme with saturating amounts of magnesium resulted in a significant modification of the enzyme stability (Figure 3A). The transitions extended from ~0.4 to 1.75 M. Analysis of the thermodynamic parameters revealed that the *cv*RTPase-Mg

Table 2. Thermodynamic unfolding parameters measured by equilibrium guanidium chloride denaturation

Protein	C_m	M	ΔC_m	m kJ/mol/M	ΔG_{Du}^0 kJ/mol	$\Delta\Delta G_{Du}^0$
<i>cv</i> RTPase	1.03		0.00	4.65	7.20	0.00
<i>cv</i> RTPase–Mg	0.66		–0.37	3.17	5.23	–1.97
<i>cv</i> RTPase–RNA	2.30		1.27	4.91	8.54	1.34
<i>cv</i> RTPase–RNA–Mg	2.28		1.25	4.49	8.48	1.28
<i>cv</i> RTPase E24A	0.93		0.00	3.01	5.80	0.00
<i>cv</i> RTPase E24A–Mg	0.97		0.04	2.79	6.08	0.28
<i>cv</i> RTPase E26A	1.35		0.00	1.38	3.64	0.00
<i>cv</i> RTPase E26A–Mg	1.40		0.05	1.10	3.97	0.33
<i>cv</i> RTPase E165A	1.60		0.00	1.06	4.20	0.00
<i>cv</i> RTPase E165A–Mg	1.64		0.08	1.30	4.43	0.23

The parameters ΔG_{Du}^0 (Gibbs free energy of unfolding in the absence of denaturant), m (cooperativity of unfolding), and C_m (midpoint concentration of denaturant required to unfold half of the protein) were determined by guanidium chloride denaturation and from the integration of the fluorescence intensity. The differences in C_m and $\Delta\Delta G_{Du}^0$ values in comparison to the unliganded proteins (*cv*RTPase and mutants) are also shown (ΔC_m and $\Delta\Delta G_{Du}^0$, respectively).

complex is thermodynamically less stable than the unliganded enzyme (Table 2). While half of the unliganded *cv*RTPase was denatured at 1.0 M Gdm-HCl, half denaturation of the protein bound to magnesium occurred at 0.7 M. The effects of magnesium on the structural stability are also highlighted by the significant differences in the values of the respective Gibbs free energies of unfolding (Table 2). Our data indicate that the Gibbs free energy of unfolding of the enzyme bound to magnesium is decreased by 1.97 kJ/mol. Overall, these results indicate that the formation of the *cv*RTPase–Mg complex destabilizes the protein architecture, rendering it more susceptible to chemical denaturation. Interestingly, the binding of cobalt ions, which does not support the catalytic activity of the enzyme, did not result in a modification of the stability of the protein (data not shown).

The effects of magnesium on the structural stability of the enzyme were also assessed by circular dichroism spectroscopy. Thermal denaturation assays were performed both in the presence and absence of magnesium, and unfolding of the enzyme was evaluated by monitoring the changes in the α -helix content of the protein (222 nm). Thermal denaturation of the unliganded *cv*RTPase initially revealed a midpoint of thermal transition (T_m) of 56.8°C (Figure 3B). Addition of saturating concentrations of magnesium (50 mM) resulted in a shift of the T_m value to 51.2°C. Evaluation of the thermodynamic parameters of unfolding confirmed that the binding of magnesium ions to the *cv*RTPase reduces the structural stability of the enzyme (Supplementary Table 1). Note that all of the denaturation assays, performed either with increasing Gdm-HCl concentrations or by thermal denaturation, revealed monophasic unfolding curves, suggestive of a two-state unfolding model. No intermediate form could be detected during the unfolding process.

Structural and mechanistic implications

While our unfolding analyses confirmed that the binding of magnesium to the *cv*RTPase reduces the structural stability of the enzyme, the circular dichroism assays indicated that the binding of metal ions results in a minimal perturbation of the tertiary structure of the

protein. This raises questions about the conformational changes that are required for the formation of the active site of the *cv*RTPase. In order to address this issue, spectroscopic analyses were performed to determine if binding of RNA could result in a modification of the *cv*RTPase structure. Circular dichroism analyses were carried out to monitor potential structural modifications that could occur in the *cv*RTPase upon RNA binding. Note that a 5'-hydroxyl RNA substrate was used in this assay because the addition of magnesium to a classical 5'-triphosphorylated RNA would result in the hydrolysis of the substrate and its concomitant release from the active site of the enzyme. Preliminary assays were therefore performed to evaluate the concentrations of RNA required for optimal binding (Supplementary Figure 3). As can be seen in Figure 4A, analysis of the CD spectra revealed that the protein incubated with both RNA and magnesium displayed a different tertiary structure than the unliganded enzyme (Figure 4A). We then tested the effect of RNA binding on the stability of the enzyme using Gdm-HCl-induced denaturation and a significant modification of the protein stability was observed (Figure 4B). The Gibbs free energy of unfolding of the *cv*RTPase bound to RNA was thus determined (Table 2). Our data indicate that the Gibbs free energy of unfolding of the protein bound to RNA is increased by 1.34 kJ/mol. To determine if the magnesium could act by stabilizing the ground state binding of the substrate, denaturation studies were performed in the presence of a 5'-hydroxyl-terminated RNA substrate. The denaturation assays revealed that the binding of the RNA substrate is not affected by the presence of Mg^{2+} ions (Figure 4B and Table 2). We conclude that magnesium is not involved in the stabilization of the ground state binding of the RNA substrate. Note that similar conclusions were reached when the denaturation assays were performed with a 5'-diphosphorylated RNA substrate (data not shown).

Mutational analysis

Analysis of the crystal structure of the closely related yeast RNA triphosphatase revealed the presence of

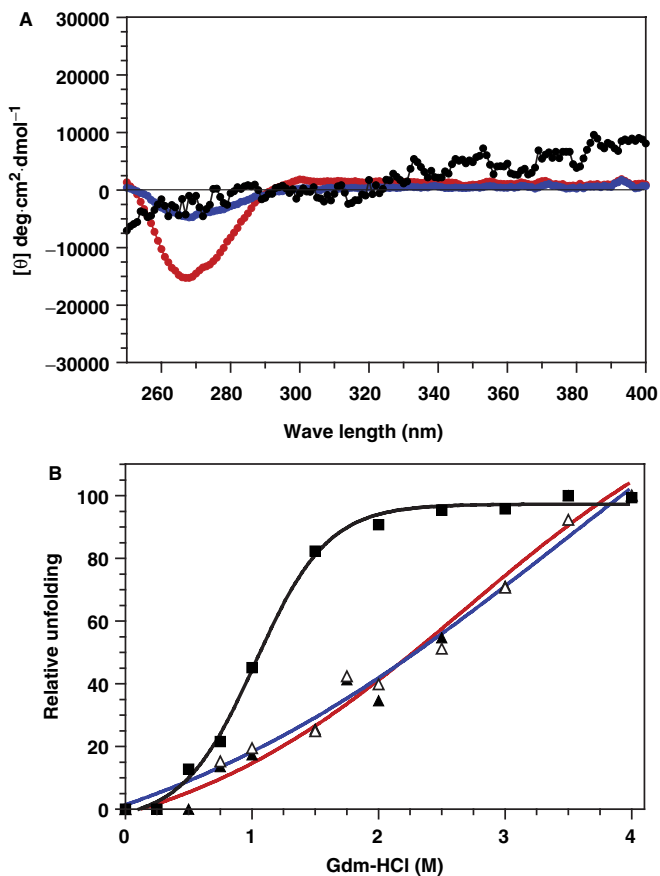


Figure 4. Consequences of substrate binding on the *cvRTPase*. (A) Near-UV circular dichroism spectra were recorded for the unliganded *cvRTPase* (black line) or the protein incubated in the presence of 20 μM RNA (blue line). The enzyme was also incubated in the presence of 20 μM RNA and 50 mM MgCl_2 (red line). In each case the enzyme concentration was 2 μM and the spectra were recorded from 250 to 400 nm. The average of six wavelength scans is presented. (B) Gdm-HCl-induced unfolding equilibrium of the *cvRTPase*. Transition curves for Gdm-HCl-induced unfolding of the unliganded *cvRTPase* (filled square, black line) or the protein incubated in the presence of 20 μM RNA (open triangle, blue line). The *cvRTPase* was also incubated in the presence of 20 μM RNA and 50 mM MgCl_2 (filled triangle, red line). Equilibrium unfolding transitions were monitored by integration of the fluorescence intensity.

a single metal ion which is coordinated by three glutamate (Glu-305, Glu-307 and Glu-496) located in the active center of the enzyme (19). Previous mutational studies have shown that these glutamate residues, as well as the corresponding amino acids of the *cvRTPase* (Glu-24, Glu-25 and Glu-165), are essential for the triphosphatase activity suggesting that these residues are likely involved in the coordination of the metal ion (23,24,33). In order to further investigate the metal ion binding activity of the *cvRTPase*, we synthesized a series of three enzymatic mutants. *Glu-24*, *Glu-26* and *Glu-165* were substituted for alanine, and the mutant polypeptides were expressed and purified in parallel with the wild-type enzyme. Note that all three mutations elicited a 100-fold decrease in RNA triphosphatase activity as judged from the release of inorganic phosphatate from a radiolabeled 5'-triphosphate RNA substrate (Supplementary Figure 4).

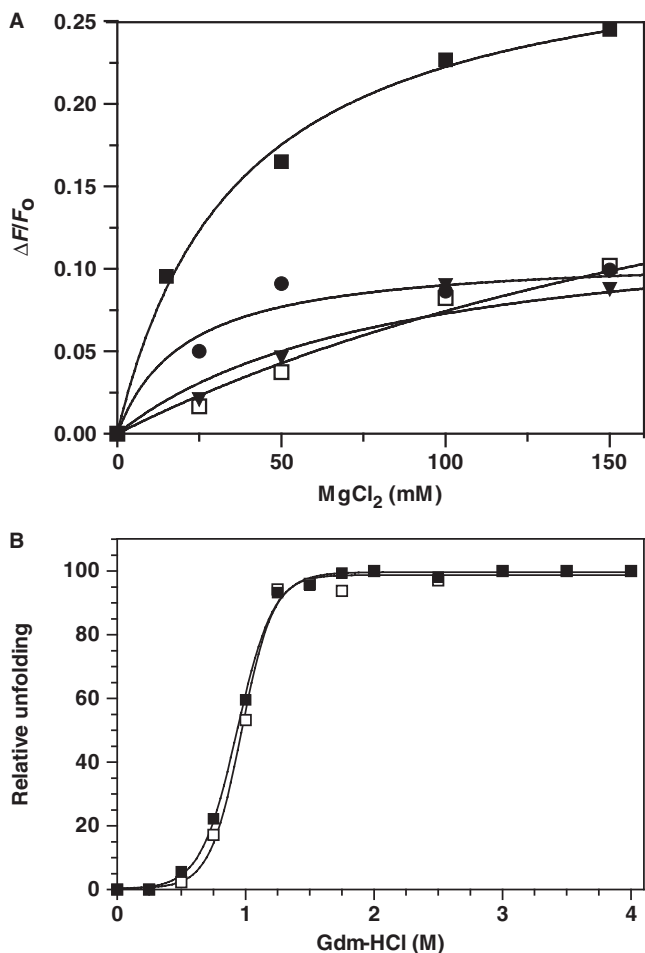


Figure 5. Characterization of the *cvRTPase* alanine mutants. (A) Fluorescence spectroscopy was used to monitor the binding of magnesium to the different *cvRTPase* mutants. Assays were performed by incubating the wild-type *cvRTPase* (filled square), E24A (filled inverted triangle), E26A (filled circle) and E165A (open square) mutants (2 μM) with increasing amounts of MgCl_2 . Excitation was performed at 290 nm, and emission was monitored from 310 to 440 nm. The saturation isotherms were generated by plotting the change in the fluorescence intensity at 333 nm as a function of added magnesium. (B) Transition curves for GdmHCl-induced unfolding of the unliganded E24A mutant (filled square), and the mutant in the presence of 50 mM of MgCl_2 (open square), were determined. Equilibrium unfolding transitions were monitored by integration of the fluorescence intensity.

The effects of single alanine mutations on the metal ion binding activity were then investigated by fluorescence spectroscopy. Substitution of Glu-24 and Glu-165 by alanine resulted in a significant decrease in the ability of the enzyme to bind magnesium (13% and 10% of the wild-type activity, respectively) (Figure 5A). However, substitution of the Glu-26 residue by alanine had a less pronounced impact on the magnesium-binding activity (30% of the wild-type activity) (Figure 5A). We conclude that each of the three glutamate residues (Glu-24, Glu-26 and Glu-165) is involved in metal ion binding. The effects of these single alanine mutations on the stability of the *cvRTPase* were then investigated by Gdm-HCl denaturation. In contrast to the wild-type enzyme, no significant

decrease in structural stability was observed when the E24A mutant was incubated with magnesium (Figure 5B). Similar results were obtained for both the E26A and E165A mutants (data not shown). Overall, our mutagenesis studies revealed the importance of three glutamate residues for the binding of magnesium and confirmed that the binding of magnesium ions to the *cv*RTPase reduces the structural stability of the enzyme.

DISCUSSION

In the present study, we extended our analyses on the role(s) of metal ions in the RNA triphosphatase reaction by monitoring the effects of magnesium binding on the *cv*RTPase, the smallest member of the metal-dependent RNA triphosphatases family. The use of fluorescence spectroscopy allowed us to precisely quantitate, for the first time, the thermodynamic parameters associated with the binding of magnesium ions to an RNA triphosphatase. Our thermodynamic analyses indicate that the initial association of magnesium with the *cv*RTPase is dominated by a favorable entropic effect. Such entropic changes can result from the release of either ions or water molecules to the bulk solvent upon ligand binding and/or from conformational changes upon complex formation (34). Although we detected minor conformational changes upon magnesium binding, the use of circular dichroism clearly demonstrated that these modifications are not significant. This suggests that the release of ions or water molecules is most likely occurring upon magnesium binding. As evidenced from the binding assays performed in the presence of neutral solutes, the interaction of the enzyme with magnesium was clearly accompanied by the release of water molecules from the enzyme. Moreover, the release of water molecules from the protein caused a concomitant favorable increase in the free energy of binding indicating the binding is accompanied by the removal of water molecules from the vicinity of the binding site supporting the involvement of water release during the binding of magnesium to the *cv*RTPase. Note that control experiments in which the effects of glycerol and ethylene glycol on the structure of the *cv*RTPase were investigated by circular dichroism and revealed that the structure of the enzyme remains unaltered in the presence of high concentrations of the solutes (Supplementary Figure 4). This rules out the possibility that the solutes can modify the structure of the enzyme under the conditions used in our assays thereby indirectly contributing to the release of water molecules. In fact, numerous structural studies have previously shown that both glycerol and ethylene glycol are generally excluded from macromolecular surfaces, and they do not interact with proteins nor do they alter their conformation (35–41).

The stoichiometry of the magnesium ion required for the RNA triphosphatase activity is an important variable to consider for the mechanistic understanding of the RNA triphosphatase reaction. The binding assays performed in the present study provide no indication on the precise number of metal ions required for catalytic

activity. Our data clearly indicate that the *cv*RTPase can bind magnesium in the absence of the RNA substrate. Moreover, a Scatchard plot of magnesium binding is linear, providing no evidence for multiple classes of independent magnesium ion binding sites, nor of cooperative binding sites (Supplementary Figure 1B). However, the binding of additional metal ions upon RNA binding cannot be excluded. It is possible that additional metal-binding sites are present in the enzyme-substrate complex. In fact, a two-metal mechanism has recently been proposed based on synergistic activation of the enzyme by manganese and magnesium for both the baculovirus LEF4 RNA triphosphatase and the trypanosome RNA triphosphatase (42,43). It has been suggested that one metal could be coordinated by three glutamates while the second metal might entail contacts with the α and β phosphates of the RNA substrate (43). Based on crystallographic analysis of the yeast RNA triphosphatase, a one-step in-line catalytic mechanism has previously been proposed in which the single metal ion coordinated by the glutamate residues emanating from the floor of the tunnel (Glu305, Glu307 and Glu496), promotes catalysis by stabilizing a pentacoordinate phosphorane transition state (19). However, additional roles in the reaction chemistry, such as substrate coordination, stabilization of the intermediate transition state or activation of nucleophiles, cannot be excluded. A likely role for the potential metal ion bound to the RNA substrate could be in the stabilization of the substrate for optimal orientation with the catalytic side chains of the enzyme. It is interesting to note that such a stabilizing effect has recently been noted for the yeast RNA triphosphatase (25). The fact that the hydrolysis of RNA triphosphate ends by *cv*RTPase is activated by magnesium, but not by manganese or cobalt, while the NTPase activity is supported by manganese and cobalt, highlights the importance of the metal ion cofactors in catalysis (23). Based on the results of the present study, we hypothesize that the binding of magnesium ions probably induces local conformational perturbations in the active site residues that ultimately positions the lateral chains of critical amino acids involved in catalysis.

A single metal ion is present in the crystal structure of the closely related yeast RNA triphosphatase (19). This ion is coordinated by three glutamate (Glu-305, Glu-307 and Glu-496) located in the active center of the enzyme (19). Previous mutational studies have shown that these glutamate residues are essential for the triphosphatase activity suggesting that these residues are likely involved in the coordination of the metal ion (33). Similar mutational studies performed on the corresponding residues of the *cv*RTPase (Glu-24, Glu-26 and Glu-165) also revealed the importance of these residues for catalytic activity (22,23). Using a combination of fluorescence spectroscopy and denaturation studies, the present mutational analysis clearly confirmed that each of these glutamate residues is involved in the binding of the metal ion. The informative finding is that the binding of magnesium to these catalytically defective mutants is severely decreased but not entirely abrogated. Analysis of the crystal structure of the yeast RNA triphosphatase

revealed that the metal ion is involved in a number of different interactions (19). The six coordination sites of the metal ion are entirely occupied through interactions with glutamate residues (three sites), two water molecules (two sites) and a sulfate ion (one site), which mimics the hydrolyzed γ phosphate generated during the phosphohydrolase reaction (19). We therefore hypothesize that binding of magnesium in the absence of one of the three glutamate residues is not entirely abrogated because the coordination sites of the metal ion can still be occupied through interactions with other partners. However, since these mutants are catalytically defective, this indicates that the active center of *cv*RTPase is intolerant to virtually any perturbations of the metal coordination sphere, highlighting the critical role of the enzyme-bound metal ions.

The *cv*RTPase is more closely related to the cellular RNA triphosphatases of fungi (*S. cerevisiae*) than to other DNA virus-encoded RNA triphosphatases. For instance, the *cv*RTPase is encoded by a separate polypeptide (as in yeast) while DNA viruses encode a multifunctional enzyme in which the RNA triphosphatase and RNA guanylyltransferase activities are linked in *cis* on a single protein (2). Moreover, sequence alignments suggest that its active site is located within a topological tunnel likely to be similar to that of *S. cerevisiae*, and mutational studies have confirmed that most amino acids involved in catalysis are similar in both enzymes (22,23,33). However, several differences in structure-activity relationships clearly indicated that the two enzymes vary in their reliance on certain residues for their respective activities (24). This is perhaps not surprising as the *cv*RTPase lacks several structural elements that are found on the corresponding yeast enzyme (24). These elements include the RNA guanylyltransferase-binding site, a dimerization interface and an α -helix found on the lateral surface of the yeast enzyme. The current study contributes to highlight additional differences between the two related enzymes. For instance, previous denaturation studies performed on the yeast RNA triphosphatase clearly demonstrated that magnesium is involved in the stabilization of the ground state binding of the RNA substrate and involve interactions unrelated to those at the scissile phosphate or specific to the transition state (25). However, such stabilizing effects were clearly not observed upon magnesium binding to the *cv*RTPase. Moreover, addition of magnesium to the *cv*RTPase in the absence of the RNA substrate led to a significant decrease in structural stability, a property that is not shared by the yeast enzyme (25). Finally, structural modifications were noted in the *cv*RTPase upon RNA binding while our previous structural studies performed on the yeast enzyme revealed that the enzyme does not undergo conformational changes upon RNA binding (25). Interestingly, stability and structural studies have also been performed on the more distantly related RNA triphosphatases of the parasitic protozoa *Trypanosoma cruzi* and *Trypanosoma brucei* (44). Metal ion-binding studies showed that the stability of the *T. cruzi* enzyme is increased in the presence of metal ion while the stability of the *T. brucei* enzyme remained stable following the binding of metal ions (44). In fact,

denaturation studies demonstrated that the *T. brucei* enzyme remains stable in the absence of the metal ion. This stability of the *T. brucei* enzyme has been attributed to its high content in cysteine residues, although other structural constraints are probably contributing to the stability of the enzyme. Clearly, differences between the members of the metal-dependent RNA triphosphatases are starting to emerge, and the future determination of additional crystal structures should provide additional clues on the reaction chemistry. This is further emphasized by the recent characterization of a novel triphosphatase activity found in *Clostridium thermocellum*. Although metal ions are required for the phosphohydrolase activity of the protein, mutational studies indicate that distinct molecular determinants are involved in both substrate-specificity and structure-activity relationships of different related triphosphatases.

SUPPLEMENTARY DATA

Supplementary Data are available at NAR Online.

ACKNOWLEDGEMENTS

We thank Dr James Van Etten for the generous gift of the *Chlorella* virus DNA. This work was supported by a grant from the Canadian Institutes for Health Research (CIHR). The RNA group is supported by a grant from the CIHR and by the Université de Sherbrooke. M.B. is a New Investigator Scholar from the CIHR, and J.P.P. holds the Canada Research Chair in Genomics and Catalytic RNA. Both M.B. and J.P.P. are members of the Infectious diseases group of the Centre de Recherche Clinique Étienne-Lebel. Funding to pay the Open Access publication charges for this article was provided by the CIHR.

Conflict of interest statement. None declared.

REFERENCES

1. Furuichi, Y. and Shatkin, A.J. (2000) Viral and cellular mRNA capping: past and prospects. *Adv. Virol. Res.*, **55**, 135–184.
2. Shuman, S. (2000) Structure, mechanism, and evolution of the mRNA capping apparatus. *Prog. Nucleic Acids Res. Mol. Biol.*, **66**, 1–40.
3. Bisailon, M. and Lemay, G. (1997) Viral and cellular enzymes involved in synthesis of mRNA cap structure. *Virology*, **236**, 1–7.
4. Luongo, C.L., Reinisch, K.M., Harrison, S.C. and Nibert, M.L. (2000) Identification of the guanylyltransferase region and active site in reovirus mRNA capping protein lambda2. *J. Biol. Chem.*, **275**, 2804–2810.
5. Bisailon, M. and Lemay, G. (1997) Characterization of the reovirus lambda1 protein RNA 5'-triphosphatase activity. *J. Biol. Chem.*, **272**, 29954–29957.
6. Gross, C.H. and Shuman, S. (1998) RNA 5'-triphosphatase, nucleoside triphosphatase, and guanylyltransferase activities of baculovirus LEF-4 protein. *J. Virol.*, **72**, 10020–10028.
7. Myette, J.R. and Niles, E.G. (1996) Characterization of the vaccinia virus RNA 5'-triphosphatase and nucleotide triphosphate phosphohydrolase activities. Demonstration that both activities are carried out at the same active site. *J. Biol. Chem.*, **271**, 11945–11952.

8. Benzaghou, I., Bougie, I., Picard-Jean, F. and Bisailon, M. (2006) Energetics of RNA binding by the West Nile virus RNA triphosphatase. *FEBS Lett.*, **580**, 867–877.
9. Vasiljeva, L., Merits, A., Auvinen, P. and Kaariainen, L. (2000) Identification of a novel function of the alphavirus capping apparatus. RNA 5'-triphosphatase activity of Nsp2. *J. Biol. Chem.*, **275**, 17281–17287.
10. Ho, C.K., Van Etten, J.L. and Shuman, S. (1996) Expression and characterization of an RNA capping enzyme encoded by *Chlorella* virus PBCV-1. *J. Virol.*, **70**, 6658–6664.
11. Bougie, I. and Bisailon, M. (2004) The broad spectrum antiviral nucleoside ribavirin as a substrate for a viral RNA capping enzyme. *J. Biol. Chem.*, **279**, 22124–22130.
12. Liuzzi, M., Mason, S.W., Cartier, M., Lawetz, C., McCollum, R.S., Dansereau, N., Bolger, G., Lapeyre, N., Gaudette, Y. et al. (2005) Inhibitors of respiratory syncytial virus replication target cotranscriptional mRNA guanylation by viral RNA-dependent RNA polymerase. *J. Virol.*, **79**, 13105–13115.
13. Ho, C.K., Pei, Y. and Shuman, S. (1998) Yeast and viral RNA 5' triphosphatases comprise a new nucleoside triphosphatase family. *J. Biol. Chem.*, **273**, 34151–34156.
14. Martins, A. and Shuman, S. (2000) Mechanism of phosphoanhydride cleavage by baculovirus phosphatase. *J. Biol. Chem.*, **275**, 35070–35076.
15. Gross, C.H. and Shuman, S. (1998) Characterization of a baculovirus-encoded RNA 5'-triphosphatase. *J. Virol.*, **72**, 7057–7063.
16. Itoh, N., Mizumoto, K. and Kaziro, Y. (1984) Messenger RNA guanylyltransferase from *Saccharomyces cerevisiae*. Catalytic properties. *J. Biol. Chem.*, **259**, 13930–13936.
17. Shuman, S. (1990) Catalytic activity of vaccinia mRNA capping enzyme subunits coexpressed in *Escherichia coli*. *J. Biol. Chem.*, **265**, 11960–11966.
18. Yamada-Okabe, T., Mio, T., Matsui, M., Kashima, Y., Arisawa, M. and Yamada-Okabe, H. (1998) Isolation and characterization of the *Candida albicans* gene for mRNA 5'-triphosphatase: association of mRNA 5'-triphosphatase and mRNA 5'-guanylyltransferase activities is essential for the function of mRNA 5'-capping enzyme *in vivo*. *FEBS Lett.*, **435**, 49–54.
19. Lima, C.D., Wang, L.K. and Shuman, S. (1999) Structure and mechanism of yeast RNA triphosphatase: an essential component of the mRNA capping apparatus. *Cell*, **99**, 533–543.
20. Changela, A., Ho, C.K., Martins, A., Shuman, S. and Mondragon, A. (2001) Structure and mechanism of the RNA triphosphatase component of mammalian mRNA capping enzyme. *EMBO J.*, **20**, 2575–2586.
21. Changela, A., Martins, A., Shuman, S. and Mondragon, A. (2005) Crystal structure of baculovirus RNA triphosphatase complexed with phosphate. *J. Biol. Chem.*, **280**, 17848–17856.
22. Van Etten, J.L. and Meints, R.H. (1999) Giant viruses infecting algae. *Annu. Rev. Microbiol.*, **53**, 447–494.
23. Ho, C.K., Gong, C. and Shuman, S. (2001) RNA triphosphatase component of the mRNA capping apparatus of *Paramecium bursaria* *Chlorella* virus 1. *J. Virol.*, **75**, 1744–1750.
24. Gong, C. and Shuman, S. (2002) *Chlorella* virus RNA triphosphatase. Mutational analysis and mechanism of inhibition by tripolyphosphate. *J. Biol. Chem.*, **277**, 15317–15324.
25. Bisailon, M. and Bougie, I. (2003) Investigating the role of metal ions in the catalytic mechanism of the yeast RNA triphosphatase. *J. Biol. Chem.*, **278**, 33963–33971.
26. Bougie, I. and Bisailon, M. (2006) Inhibition of a metal-dependent viral RNA triphosphatase by decavanadate. *Biochem. J.*, **398**, 557–567.
27. Pace, C.N. (1995) Evaluating contribution of hydrogen bonding and hydrophobic bonding to protein folding. *Methods Enzymol.*, **259**, 538–554.
28. Eftink, M.R. and Ghiron, C.A. (1981) Fluorescence quenching studies with proteins. *Anal. Biochem.*, **114**, 199–227.
29. Swaminathan, C.P., Nandi, A., Visweswariah, S.S. and Suroliya, A. (1999) Thermodynamic analyses reveal role of water release in epitope recognition by a monoclonal antibody against the human guanylyl cyclase C receptor. *J. Biol. Chem.*, **274**, 31272–31278.
30. Painter, G.R., Wright, L.L., Hopkins, S. and Furman, P.A. (1991) Initial binding of 2'-deoxynucleoside 5'-triphosphates to human immunodeficiency virus type 1 reverse transcriptase. *J. Biol. Chem.*, **266**, 19362–19368.
31. Labowicz, J.R. (1999) *Principles of Fluorescence spectroscopy*, 2nd edn. Kluwer/Plenum, NY, pp. 237–266.
32. Caloun, D.B., Vanderkooi, J.M. and Englander, S.W. (1983) Penetration of small molecules into proteins studied by quenching of phosphorescence and fluorescence. *Biochemistry*, **22**, 1533–1539.
33. Bisailon, M. and Shuman, S. (2001) Structure-function analysis of the active site tunnel of yeast RNA triphosphatase. *J. Biol. Chem.*, **276**, 17261–17266.
34. Beaudette, N.V. and Langerman, N. (1980) The thermodynamics of nucleotide binding to proteins. *Crit. Rev. Biochem.*, **9**, 145–169.
35. Swaminathan, C.P., Suroliya, N. and Suroliya, A. (1998) Role of water in the specific binding of mannose and mannoooligosaccharides to Concanavalin A. *J. Am. Chem. Soc.*, **120**, 5153–5159.
36. Parsegian, V.A., Rand, R.P. and Rau, D.C. (1995) Macromolecules and water: probing with osmotic stress. *Methods Enzymol.*, **259**, 43–94.
37. Goldanskii, V.I. and Krupnyanskii, Y.F. (1995) Protein dynamics: hydration, temperature, and solvent viscosity effects as revealed by Rayleigh scattering of Mossbauer radiation. In Gregory, R.B. (ed), *Protein-Solvent Interactions*. Marcel Dekker Inc., NY, pp. 289–326.
38. Timasheff, S.N. (1993) The control of protein stability and association by weak interactions with water: how do solvents affect these processes? *Annu. Rev. Biophys. Biomol. Struct.*, **22**, 67–97.
39. Oliveira, A.C., Gaspar, L.P., Da Poian, A.T. and Silva, J.L. (1994) Arc repressor will not denature under pressure in the absence of water. *J. Mol. Biol.*, **240**, 184–187.
40. Prieve, A., Almagor, A., Yedgar, S. and Gavish, B. (1996) Glycerol decreases the volume and compressibility of protein interior. *Biochemistry*, **35**, 2061–2066.
41. Donovan, J.W. (1969) Changes in ultraviolet absorption produced by alteration of protein conformation. *J. Biol. Chem.*, **244**, 1961–1967.
42. Martins, A. and Shuman, S. (2001) Mapping the triphosphatase active site of baculovirus mRNA capping enzyme LEF-4 and evidence for a two-metal mechanism. *Nucleic Acids Res.*, **31**, 1455–1463.
43. Gong, C., Martins, A. and Shuman, S. (2003) Structure-function analysis of *Trypanosoma brucei* RNA triphosphatase and evidence for a two-metal mechanism. *J. Biol. Chem.*, **278**, 50843–50852.
44. Kikuti, C.M., Tersariol, I.L.S. and Schenkman, S. (2006) Divalent metal requirements for catalysis and stability of the RNA triphosphatase from *Trypanosoma cruzi*. *Mol. Biochem. Parasitol.*, **150**, 83–95.